Nanoscale

PAPER

View Article Online
View Journal | View Issue

Cite this: *Nanoscale*, 2016, **8**, 8887

Semiconducting organic–inorganic nanocomposites by intimately tethering conjugated polymers to inorganic tetrapods†

Jaehan Jung, Young Jun Yoon and Zhiqun Lin*

Semiconducting organic–inorganic nanocomposites were judiciously crafted by placing conjugated polymers in intimate contact with inorganic tetrapods *via* click reaction. CdSe tetrapods were first synthesized by inducing elongated arms from CdSe zincblende seeds through seed-mediated growth. The subsequent effective inorganic ligand treatment, followed by reacting with short bifunctional ligands, yielded azide-functionalized CdSe tetrapods (*i.e.*, CdSe–N_3). Finally, the ethynyl-terminated conjugated polymer poly(3-hexylthiophene) (*i.e.*, P3HT–≡) was tethered to CdSe–N_3 tetrapods *via* a catalyst-free alkyne–azide cycloaddition, forming intimate semiconducting P3HT–CdSe tetrapod nanocomposites. Intriguingly, the intimate contact between P3HT and CdSe tetrapod was found to not only render the effective dispersion of CdSe tetrapods in the P3HT matrix, but also facilitate the efficient electronic interaction between these two semiconducting constituents. The successful anchoring of P3HT chains onto CdSe tetrapods was substantiated through Fourier transform infrared spectroscopy and nuclear magnetic resonance spectroscopy measurements. Moreover, the absorption and photoluminescence studies further corroborated the intimate tethering between P3HT and CdSe tetrapods. The effect of the type of bifunctional ligands (*i.e.*, aryl *vs.* aliphatic ligands) and the size of tetrapods on the device performance of hybrid organic–inorganic solar cells was also scrutinized. Interestingly, P3HT–CdSe tetrapod nanocomposites produced *via* the use of an aryl bifunctional ligand (*i.e.*, 4-azidobenzoic acid) exhibited an improved photovoltaic performance compared to that synthesized with their aliphatic ligand counterpart (*i.e.*, 5-bromovaleric acid). Clearly, the optimal size of CdSe tetrapods ensuring the effective charge transport in conjunction with the good dispersion of CdSe tetrapods rendered an improved device performance. We envision that the click-reaction strategy enabled by capitalizing on two consecutive effective ligand exchanges (*i.e.*, inorganic ligand treatment and subsequent bifunctional ligand exchange) to yield intimately connected organic–inorganic nanocomposites provides a unique platform for developing functional optoelectronic devices.

Received 12th January 2016,
Accepted 24th March 2016

DOI: 10.1039/c6nr00269b

www.rsc.org/nanoscale

Introduction

Organic–inorganic nanocomposites composed of semiconductor nanocrystals (NCs) and conjugated polymers (CPs) have garnered considerable attention as they offer a promising opportunity for developing optoelectronic materials and devices due to the extensive set of advantageous and complementary characteristics of NCs and CPs, including high electron mobility and the size-dependent optical and electronic properties of NCs, in conjunction with lightweight, flexibility, low cost, and large area solution-processability of CPs.[1–5] Among CPs, poly(3-hexylthiophene) (P3HT) is one of the most extensively studied CPs as it possesses tailorable electrochemical properties, a large extinction coefficient, and high hole mobility.[6] Notably, the use of CPs as a photoactive layer in solar cells often results in low performance as their electron mobility is far behind their hole mobility, thus requiring the incorporation of electron-accepting materials such as fullerene derivatives and inorganic materials to ensure efficient charge separation and transport for high-performance devices.

Shape control of semiconducting NCs is widely recognized as an effective means of tailoring their size-dependent physical and chemical properties. This opens up exciting opportunities for a wide range of applications, including LEDs,[7] solar cells,[8,9] biosensors,[10,11] and tunable lasers.[12,13] It is worth noting that semiconducting tetrapods carry the propensity to form interconnected three-dimensional structures when

School of Materials Science and Engineering, Georgia Institute of Technology, Atlanta, GA 30332, USA. E-mail: zhiqun.lin@mse.gatech.edu

†Electronic supplementary information (ESI) available. See DOI: 10.1039/c6nr00269b

placed together due to their intrinsic three-dimensional architecture, thus providing a continuous and effective channel for efficiently transporting electrons, an advantage over spherical quantum dots (QDs) where electron hopping between QDs is required and quantum rods (QRs) where the alignment of QRs perpendicular to the electrodes is needed.

Herein, we report a facile and robust strategy for crafting semiconducting organic–inorganic nanocomposites by placing conjugated polymers in intimate contact with inorganic tetrapods *via* catalyst-free click chemistry. CdSe tetrapods with high selectivity were first synthesized by inducing elongated arms from CdSe zincblende seeds through the combination of the use of halide ligands, continuous precursor injection, and seed-mediated growth. Subsequently, oleic acid (OA)-capped CdSe tetrapods were subjected to inorganic ligand treatment to completely remove insulating fatty ligands (*i.e.*, OA), followed by introducing either 4-azidobenzoic acid or 5-bromovaleric acid as bifunctional ligands and substituting bromine of 5-bromovaleric acid into the azide, yielding azide-functionalized CdSe tetrapods (*i.e.*, CdSe–N_3). It is notable that bifunctional ligands not only act as coupling agents that anchor onto the CdSe tetrapod surface, but also introduce the desired terminal functional group for further reaction. Meanwhile, ethynyl-terminated P3HT (*i.e.*, P3HT–≡) was prepared by a quasi-living Grignard metathesis (GRIM) method. Finally, the intimate tethering of P3HT–≡ to CdSe–N_3 was rendered by catalyst-free alkyne–azide cycloaddition between them, leading to the formation of P3HT–CdSe tetrapod nanocomposites. Notably, this strategy dispenses with the need for employing metallic catalysts in click reaction, which are regarded as impurities that are detrimental to the device performance. Fourier transform infrared spectroscopy and nuclear magnetic resonance spectroscopy studies substantiated the successful anchoring of P3HT chains onto CdSe tetrapods. In addition, such intimate tethering between these two semiconducting substituents was further corroborated by absorption and photoluminescence measurements. Photovoltaic devices were fabricated using P3HT–CdSe tetrapod nanocomposites crafted based on 4-azidobenzoic acid- or 5-bromovaleric acid-capped CdSe tetrapods. Interestingly, the device produced using the aryl bifunctional ligand (*i.e.*, 4-azidobenzoic acid) exhibited an enhanced photovoltaic performance compared to that synthesized with its aliphatic ligand counterpart (*i.e.*, 5-bromovaleric acid). Furthermore, the optimal size of CdSe tetrapods ensuring the effective charge transport together with good dispersion of CdSe tetrapods was found to impart an improvement in the device performance. Clearly, in sharp contrast to CP/NC composites widely prepared by simply physically mixing them as in copious past work, which often leads to microscopic phase separation and limited performance of the resulting optoelectronic devices owing to the poor charge transfer as a direct consequence of reduced interfacial areas between CPs and NCs, the click-reaction strategy enabled by capitalizing on two consecutive effective ligand exchanges (*i.e.*, inorganic ligand treatment and the subsequent bifunctional ligand exchange) yields intimate organic–inorganic nanocomposites. As such, it imparts an effective electronic interaction at the CP/NC interface, thereby promoting the interfacial charge transfer for developing a wide range of optoelectronic devices.

Results and discussion

The synthesis of P3HT–CdSe tetrapod nanocomposites is shown in Scheme 1. It involves the ligand exchange with inorganic ligands (*i.e.*, HBF_4 in the upper panels of Scheme 1a and b), the introduction of azide functional groups (lower right panels in Scheme 1a and b), and the click reaction with ethynyl-terminated P3HT (*i.e.*, yielding the P3HT–CdSe tetrapod; lower left panels in Scheme 1a and b) in sequence. High-quality CdSe tetrapods were first synthesized by growing four arms from oleic acid (OA)-capped CdSe zincblende (ZB) quantum dot (QD) seeds *via* a continuous precursor injection method,[14] where the Cd and Se precursors were injected successively into the seed solution (*i.e.*, ZB CdSe QDs) in order to maintain the reaction conditions in the kinetic growth regime for the anisotropic growth of arms. CdSe ZB QD seeds were synthesized by employing a non-trioctylphosphine-based route, where cadmium oleate solution was added into the Se/octadecene solution.[15] It is notable that the wurtzite (WZ) phase is more favorable than ZB for the growth of anisotropic structures in order to achieve high selectivity of tetrapods. In this context, halide ligands (*i.e.*, cetyltrimethylammonium bromide (CTAB)) were also added during the injection of precursors to trigger the formation of four WZ arms that elongated from the {111} facets of the ZB seeds.[14,16] Halide ligands favor WZ formation as they selectively bind to the $(11\bar{2}0)$ and $(10\bar{1}0)$ facets of WZ arms more strongly than OA, thereby effectively replacing OA.[16] The high-resolution TEM images revealed that the four WZ arms with a diameter of 7.56 ± 0.23 nm and a length of 41 ± 2 nm were successfully grown from the CdSe ZB QD seeds of a diameter of 5.12 ± 0.16 nm under these conditions. In order to scrutinize the size effect of the tetrapod on device performance of the resulting solar cells based on P3HT–CdSe tetrapod nanocomposites as will be discussed later, CdSe tetrapods with different sizes were synthesized by controlling the amount of cadmium oleate ($Cd(OA)_2$) and Se precursors injected while using the same ZB CdSe seeds (Fig. 1a and b). The injection time t was controlled to be varied from 10 min, 50 min, to 90 min at the fixed injection rate of 0.4 ml min^{-1}. Accordingly, on the basis of TEM imaging, the arm length of OA-capped CdSe tetrapods was determined to be 10 nm (corresponding to a stacking height = 16 nm; t = 10 min), 41 ± 2 nm (stacking height = 65 nm in total; t = 50 min), and 65 nm (stacking height = 94 nm; t = 90 min) (Fig. 2).

It is noteworthy that the ligand exchange by inorganic ligands, such as molecular metal chalcogenide complexes, chalcogenide ions, and halide ligands, is a simple and effective route to completely removing the original insulating

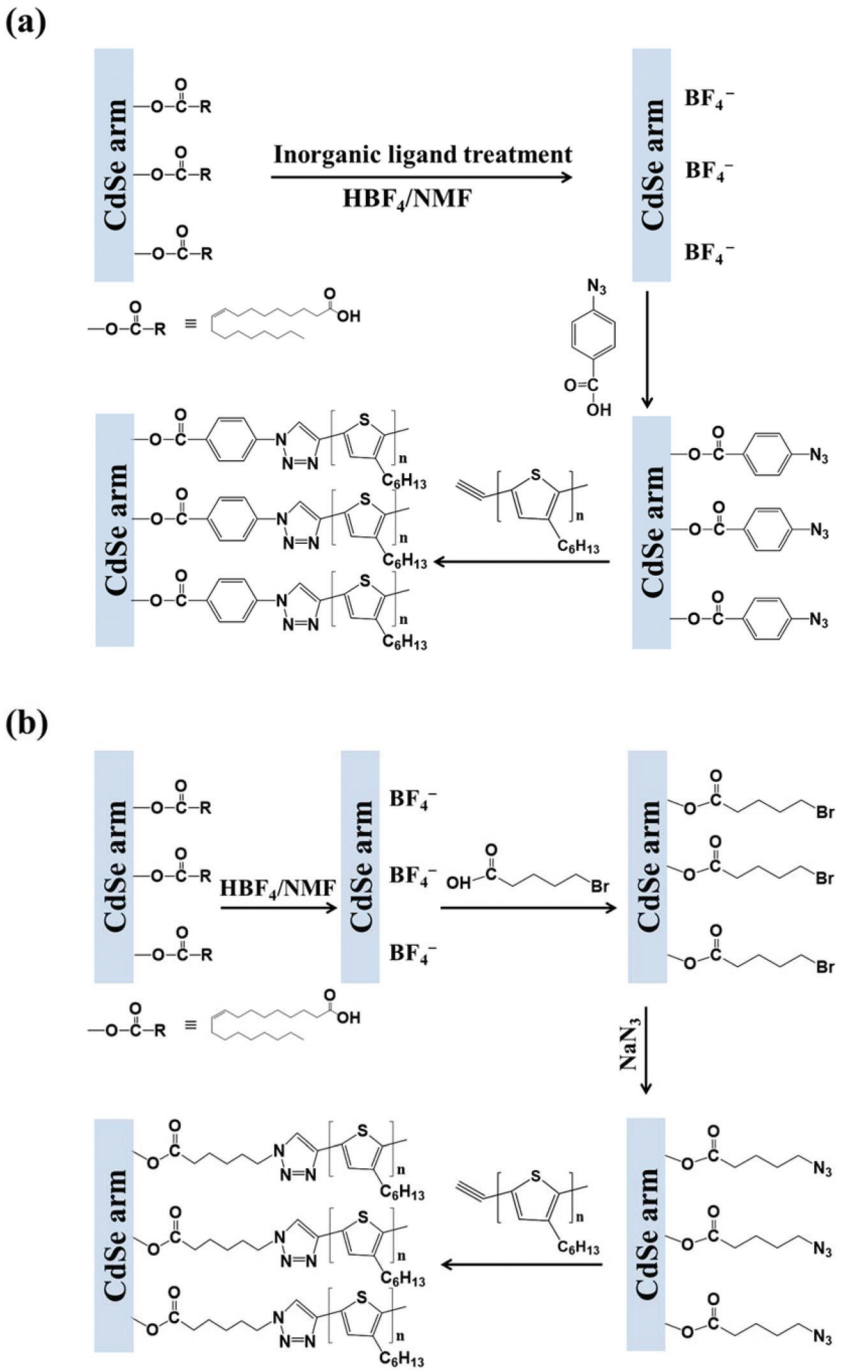

Scheme 1 Tethering ethynyl-terminated P3HT to (a) 4-azidobenzoic acid- and (b) 5-bromovaleric acid-functionalized CdSe tetrapods *via* catalyst-free click reaction, yielding P3HT–CdSe tetrapod nanocomposites, where NMF is *N*-methylformamide, and HBF_4 is fluoroboric acid. 4-Azidobenzoic acid and 5-bromovaleric acid are denoted as N_3-VA and BA, respectively.

organic ligands and introducing the desired ligand on the NC surface.[17–19] In comparison with the conventional ligand exchange approach widely using pyridine or amine to introduce the desired ligands, the ligand exchange using inorganic ligands is advantageous as it can successfully displace both covalently bonded ligands (*i.e.*, X-type) and dative bonded ligands (*i.e.*, L-type) on the NC surface, respectively.[17,20] Compared to relatively bulky insulating organic ligands (*e.g.*, OA), these inorganic ligands not only facilitate electronic interaction between NCs due to their short length, but also provide electrostatic stabilization of NC dispersions in polar solvents, thus preventing them from agglomeration.[21] In this context, despite the necessity of OA for the synthesis of well-controlled CdSe tetrapods to impart solution processability, the presence

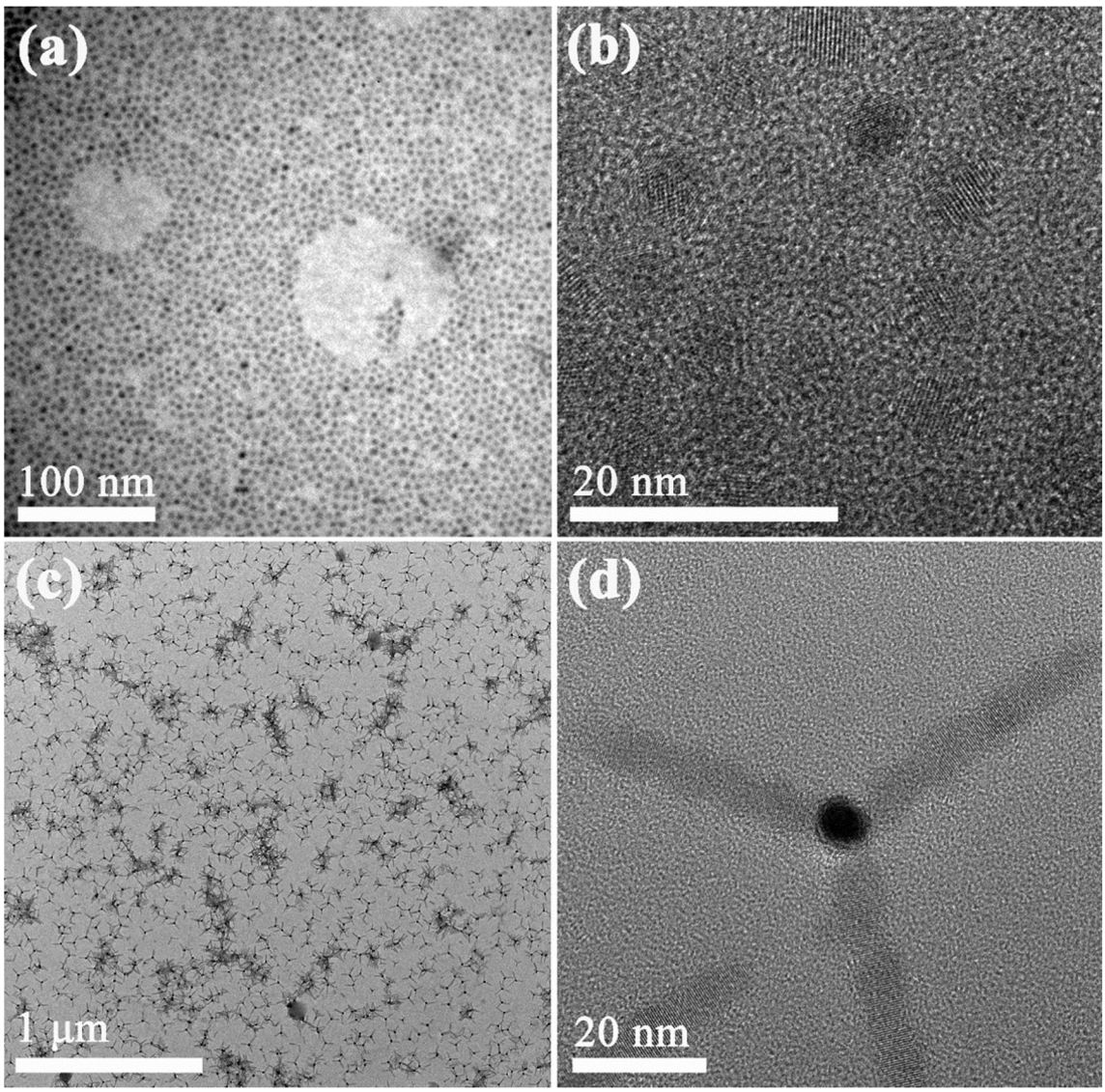

Fig. 1 TEM images of (a) oleic acid (OA)-capped zincblende CdSe QD seeds, (b) close-up of zincblende CdSe QDs, and (c, d) OA-capped CdSe tetrapods grown from OA-capped zincblende CdSe seeds.

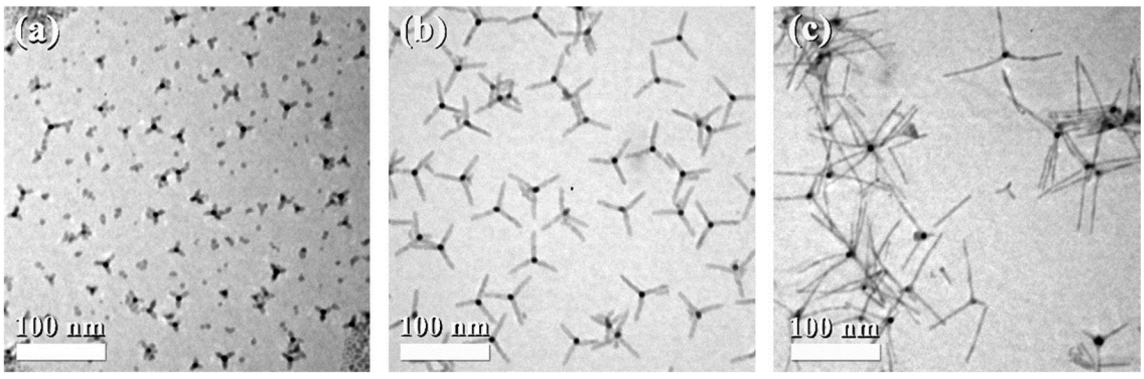

Fig. 2 TEM images of OA-capped CdSe tetrapods with the injection times of (a) 10 min, (b) 50 min, and (c) 90 min. The injection rate was fixed at 0.4 ml min^{-1}.

of OA hinders electron transport among CdSe tetrapods, especially when used in optoelectronic devices.[22,23] Thus, the OA-capped CdSe tetrapods were then treated with inorganic ligands (*i.e.*, tetrafluoroboric acid (HBF_4)) to thoroughly displace OA and form BF_4^- stabilized CdSe tetrapods (upper right panel in Scheme 1a and upper central panel in Scheme 1b).

After completely replacing insulating OA with HBF_4, aryl and aliphatic bifunctional ligands, that is, 4-azidobenzoic acid (denoted N_3-BA) and 5-bromovaleric acid (denoted VA), were introduced, respectively, onto the inorganic ion bound CdSe tetrapod surface. As such, they can be utilized as coupling agents to (i) further react with end-functionalized CPs (*i.e.*, P3HT–≡), forming P3HT–CdSe tetrapod nanocomposites, and (ii) improve the electronic interaction between CdSe tetrapods and tethered P3HT chains as the lengths of both N_3-BA and VA chains are short enough to facilitate such an interaction yet providing good dispersion of CdSe tetrapods in organic solvents due to the presence of P3HT chains on the surface.

Specifically, the mixture containing HBF_4, polar solvent (*i.e.*, *N*-methylformamide (NMF)), and OA-capped CdSe tetrapod hexane solution was vigorously shaken with vortex-mixing, thereby transferring CdSe tetrapods from the hexane phase to the NMF phase. The transfer of CdSe tetrapods occurred as the positive Cd atom sites are surrounded by BF_4^- counter ions, signifying the detachment of OA from the CdSe surface and the replacement of OA by BF_4^-. The FTIR measurements were then conducted to further verify the success of ligand exchange from OA to BF_4^- (Fig. 3a). The disappearance of the vibrational peaks from alkyl chains at 2800–3000 cm^{-1} was seen after OA was exchanged by BF_4^-.[20,24] The strong absorption of OA-capped CdSe tetrapods at 2955 cm^{-1}, 2923 cm^{-1}, and 2846 cm^{-1} can be assigned to the asymmetric C–H stretching vibrations in $-CH_3$, $-CH_2$, and the symmetric C–H stretching vibration in $-CH_2$, respectively, originating from the alkyl chain of the OA ligand.[25,26] After the HBF_4 treatment, these peaks disappeared, which is indicative of the complete removal of OA.

Subsequently, 4-azidobenzoic acid (N_3-BA) and 5-bromovaleric acid (VA) were employed as bifunctional ligands as the carboxyl acids at the one end can act as a capping agent onto the CdSe surface, and the azide group in N_3-BA and the bromine group in VA at the other end can be exploited as the coupling group for the click reaction described below. Specifically, the HBF_4-treated CdSe tetrapods were precipitated by centrifugation and re-dispersed in THF containing either N_3-BA or VA, yielding either N_3-BA-capped CdSe tetrapods (lower right panel in Scheme 1a) or VA-capped CdSe tetrapods (upper right panel in Scheme 1b). The emergence of the absorption peaks at 2959 cm^{-1}, 2923 cm^{-1}, and 2853 cm^{-1} from N_3-BA and VA indicated the capping of N_3-BA and VA on the CdSe tetrapod surface. To further confirm the ligand attachment onto the CdSe tetrapod surface, X-ray photoelectron spectroscopy (XPS) study was performed. Fig. 3b compares the binding energy of O_{1s} for N_3-BA, OA-capped CdSe tetrapods, and N_3-BA-capped CdSe tetrapods. Apparently,

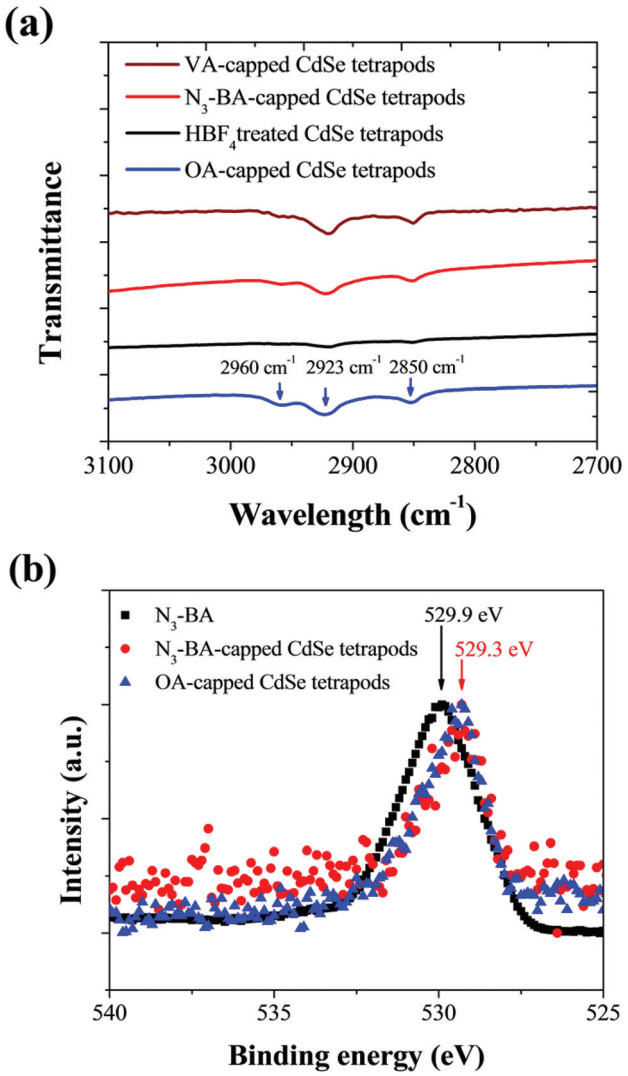

Fig. 3 (a) FTIR spectra of the as-prepared oleic acid (OA)-capped CdSe tetrapods (blue), HBF_4 treated CdSe tetrapods (black), 4-azidobenzoic acid (N_3-BA)-capped CdSe tetrapods (red), and 5-bromovaleric acid (Br-VA)-capped CdSe tetrapods (brown). (b) XPS spectra of O_{1s} binding energy for 4-azidobenzoic acid (N_3-BA; black squares), N_3-BA-capped CdSe tetrapods (red circles), and OA-capped CdSe tetrapods (blue triangles).

the peaks of binding energy between N_3-BA and N_3-BA-capped CdSe tetrapods differed by approximately 0.6 eV. This 0.6 eV shift can be rationalized by the difference in electron density of oxygen atoms resulting from the binding of N_3-BA ligands to the CdSe surface, suggesting success in anchoring N_3-BA onto CdSe tetrapods.

For VA-capped CdSe tetrapods, the bromine moiety of the VA ligand capped on the CdSe tetrapods were converted into the azide group by reacting with sodium azide (NaN_3) in THF, forming N_3-VA-capped CdSe tetrapods (lower right panel in Scheme 1b). Finally, both azide-functionalized CdSe tetrapods, that is, N_3-BA-capped and N_3-VA-capped CdSe tetrapods, were grafted with ethynyl-terminated P3HT (*i.e.*, P3HT–≡) *via* catalyst-free click chemistry, yielding P3HT–CdSe tetrapod

nanocomposites (lower left panel in Scheme 1a and lower left panel in Scheme 1b, respectively). The success of coupling of two semiconducting constituents was substantiated by FTIR and ^{1}H NMR measurements. Fig. 4 compares FTIR spectra of bare CdSe tetrapods (*i.e.*, BF_4^- stabilized CdSe tetrapods), N_3-functionalized CdSe tetrapods (*i.e.*, N_3-BA-capped CdSe tetrapods (Fig. 4a) and N_3-VA-capped CdSe tetrapods (Fig. 4b)), and P3HT–CdSe tetrapod nanocomposites (Fig. 4a and b). The absorption peaks at 2955 cm^{-1}, 2923 cm^{-1}, and 2846 cm^{-1} were assigned to the asymmetric C–H stretching vibrations in $-CH_3$, $-CH_2$, and the symmetric C–H stretching vibration in $-CH_2$, respectively, from the alkyl side chains in P3HT and ligands.[13,16] Obviously, the characteristic peak assigned to $-N_3$ vibration also appeared at 2040 cm^{-1} for both N_3-BA-capped CdSe tetrapods and N_3-VA-capped CdSe tetrapods. This peak was then greatly reduced after the N_3-BA-capped CdSe tetrapods and N_3-VA-capped CdSe tetrapods were coupled with P3HT–≡, signifying the successful grafting of P3HT chains onto CdSe tetrapods through 1,3-dipolar cycloaddition between the ethynyl group (*i.e.*, ≡) in P3HT–≡ and the azide group (*i.e.*, N_3) in N_3-functionalized CdSe tetrapods (*i.e.*, both N_3-BA-capped and N_3-VA-capped CdSe; referred to as CdSe–N_3). In addition, the ^{1}H NMR measurements (Fig. 5) also strongly suggested the occurrence of grafting between P3HT–≡ and CdSe–N_3 tetrapods. A proton signal at 3.5 ppm from ≡ at the

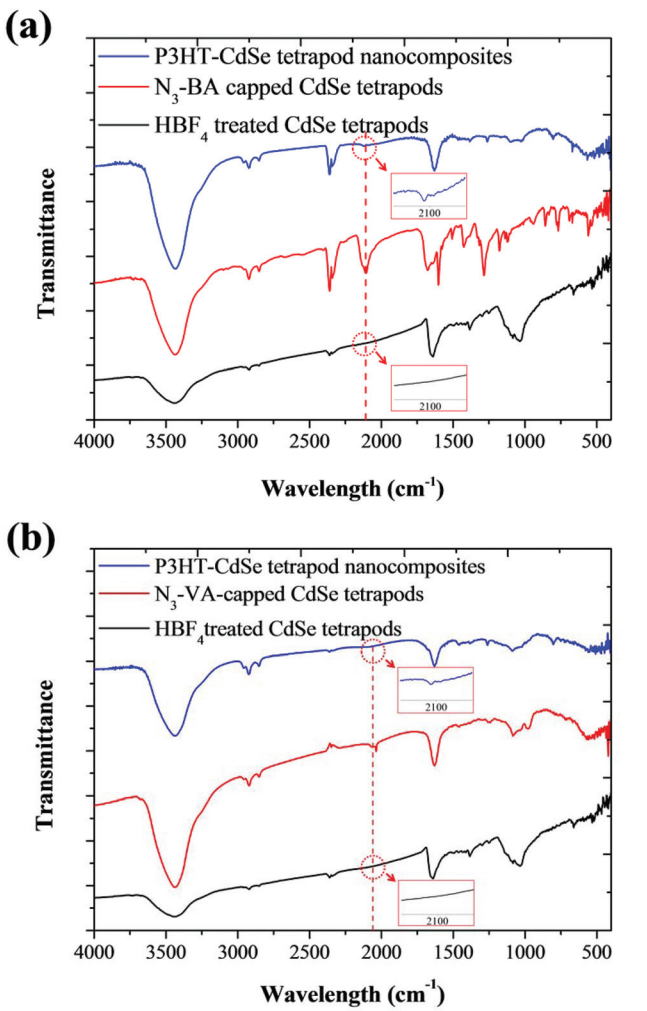

Fig. 4 FTIR spectra of (a) HBF_4 treated CdSe tetrapods (black), 4-azidobenzoic acid (N_3-BA)-capped CdSe tetrapods (red), and the resulting P3HT–CdSe tetrapod nanocomposites (blue). (b) HBF_4 treated CdSe tetrapods (black), 5-azidovaleric acid (N_3-VA)-capped CdSe tetrapods (red), and the resulting P3HT–CdSe tetrapod nanocomposites (blue).

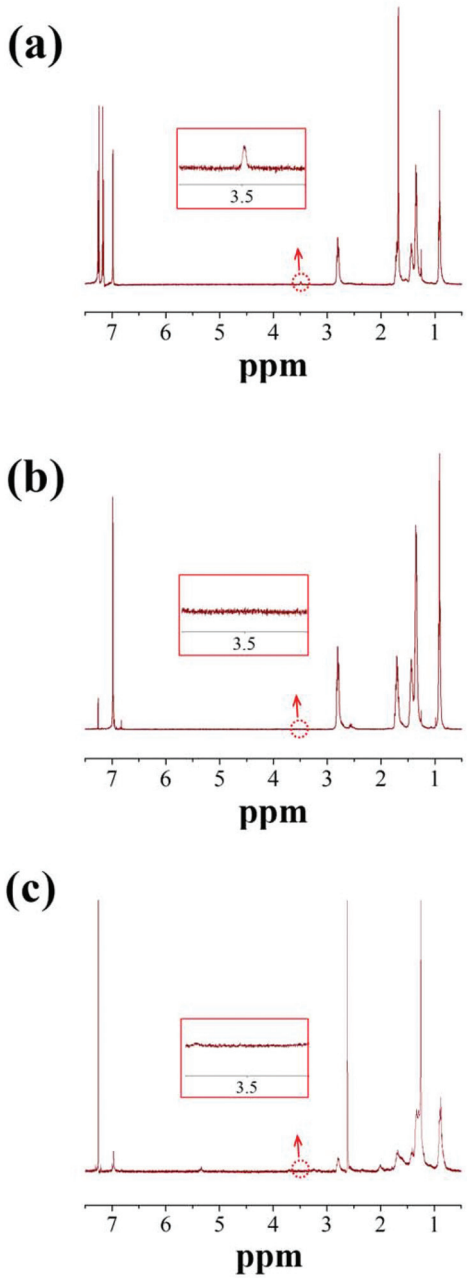

Fig. 5 ^{1}H NMR spectra of (a) ethynyl-terminated P3HT and P3HT–CdSe tetrapod nanocomposites prepared by tethering ethynyl-terminated P3HT to (b) N_3-BA-CdSe tetrapods. ^{1}H NMR spectrum of (c) N_3-VA-CdSe tetrapods. The inset is the close-ups of spectra at around 3.5 ppm.

P3HT chain end (Fig. 5a) was not observed in the P3HT–CdSe tetrapod nanocomposites after coupling P3HT–≡ with both N_3-BA-capped and N_3-VA-capped CdSe tetrapods as shown in Fig. 5b and c, respectively.

The optical properties of P3HT–≡, CdSe–N_3 tetrapods, and P3HT–CdSe tetrapod nanocomposites were then explored by UV-vis absorption and photoluminescence (PL) spectroscopy. The absorption spectra of P3HT–≡, N_3-BA-capped CdSe tetrapods, and the resulting P3HT–CdSe tetrapod nanocomposites in THF are shown in Fig. 6a. The absorption maxima of P3HT–≡ and N_3-BA-capped CdSe tetrapods were at 450 nm and 652 nm, respectively. Obviously, the absorption spectrum of the resulting P3HT–CdSe tetrapod nanocomposites was a simple superposition of the two constituents. The PL spectra of P3HT–≡, simple physical mixture composed of P3HT–≡ and N_3-BA-capped CdSe tetrapods (*i.e.*, P3HT/CdSe tetrapods), and P3HT–CdSe tetrapod nanocomposites prepared by click chemistry as described above were measured (Fig. 6c). We note that the weight ratio of CdSe tetrapods to P3HT was set to be the same in both the physical mixture of P3HT/CdSe tetrapods and P3HT–CdSe tetrapod nanocomposites, as verified by UV-vis spectroscopy measurements (Fig. 6b). Comparing to the pristine P3HT homopolymer, the quenching of PL in the physical mixture of P3HT/CdSe tetrapods and P3HT–CdSe tetrapod nanocomposites was observed (Fig. 6c), signifying the efficient charge transfer from electron-donating P3HT to electron-accepting CdSe tetrapods.[27] Intriguingly, the quenching of PL in P3HT–CdSe tetrapod nanocomposites was much pronounced in comparison with that of the physical mixture of the P3HT/CdSe tetrapod at the same weight ratio, corroborating the success of coupling between P3HT and CdSe tetrapods. Clearly, this observation further confirmed the intimate contact between P3HT and CdSe tetrapods. We note that some studies on physical[24] and chemical[26,28–30] means of achieving close contact between the conjugated polymer (CP) and the nanocrystal (NC) to yield CP–NC nanocomposites have been demonstrated, where a large fraction of residual aliphatic insulating ligands still exists on the NC surface and thus hinders the charge transport in the photoactive layer when employed in optoelectronic devices. In sharp contrast, the present study rendered the CdSe tetrapod surface purely covered with P3HT chains, *i.e.*, without any remaining insulating OA ligands as they were completely exchanged by $BF4^-$ *via* inorganic ligand treatment (Scheme 1). It is not surprising that the nanocomposites crafted *via* click reaction of P3HT–≡ and N_3-VA-capped CdSe tetrapods exhibited similar quenching behavior as the nanocomposites described above.

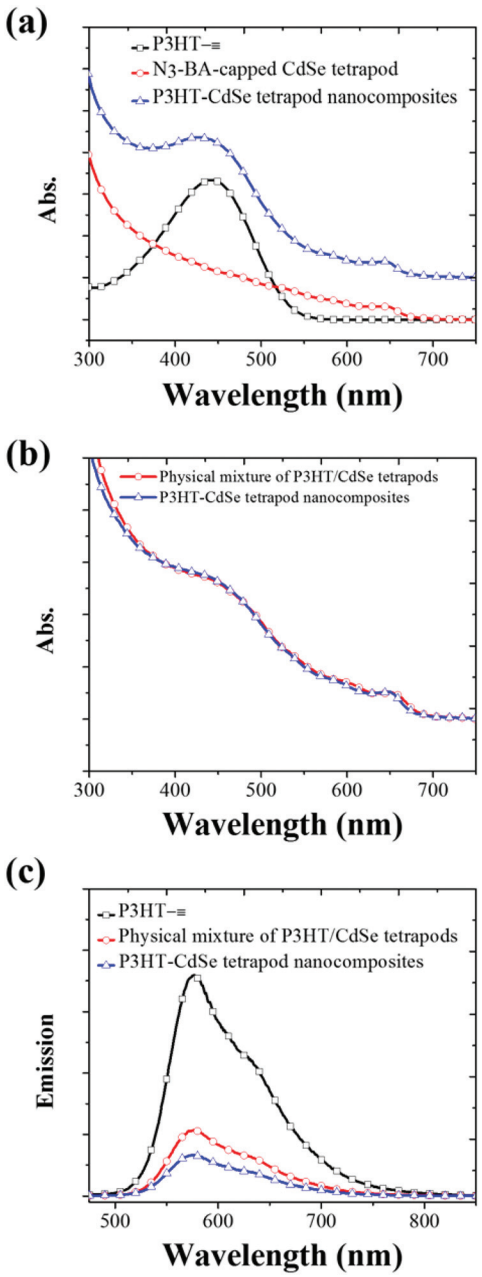

Fig. 6 (a) Absorption spectra of ethynyl-terminated P3HT (black), N_3-BA-capped CdSe tetrapods (red), and the resulting P3HT–CdSe tetrapod nanocomposites (blue) synthesized by click reaction. (b) UV-vis spectra of the physical mixture composed of P3HT/CdSe tetrapods (blue) and P3HT–CdSe tetrapod nanocomposites (red). (c) Photoluminescence spectra of ethynyl-terminated P3HT (black squares), physical mixture of P3HT/CdSe tetrapod (red circles), and P3HT–CdSe tetrapod nanocomposites (blue triangles).

In stark contrast to isotropic quantum dots (QDs) where electron hopping between QDs is needed and quantum rods (QRs) where the alignment of QRs normal to the electrodes is vital, in this study CdSe tetrapods were utilized as electron acceptors due to their intrinsic three-dimensional architecture that facilitates a continuous and effective pathway for efficient charge transport for use in organic–inorganic hybrid solar cells. Moreover, the increased interfacial area resulting from the elongated shape of the tetrapod can maximize the possibility of exciton dissociation. Finally, the ability to chemically tether P3HT on the CdSe tetrapod surface promotes the electronic interaction between P3HT and CdSe tetrapod and imparts a uniform dispersion of CdSe tetrapods in the P3HT matrix (*i.e.*, the P3HT chains tethered on the surface of

tetrapods). Thus, hybrid photovoltaic devices were fabricated by employing intimate P3HT–CdSe tetrapod nanocomposites as a photoactive layer. It should be noted that devices fabricated using the as-synthesized P3HT–CdSe tetrapod nanocomposites exhibited enhanced performance compared to those by simple physical mixture (Fig. S1†). The influence of tetrapod size and the type of bifunctional ligands (*i.e.*, 5-bromovaleric acid and 4-azidobenzoic acid) on device performance were scrutinized. First, the photovoltaic performance of devices fabricated using P3HT–CdSe tetrapod nanocomposites prepared by coupling P3HT–≡ with N_3-BA-capped CdSe tetrapods (referred to as 4-azidobenzoic acid-based devices) as well as N_3-VA-capped CdSe tetrapods (referred to as 5-bromovaleric acid-based devices) were compared. It is notable that aromatic molecules carry better charge transport properties than aliphatic molecules.[31–33] In this work, all devices were fabricated by spin-coating from the 20 mg ml^{-1} nanocomposite solution containing 20% chlorobenzene by volume in chloroform, and then thermally annealed at 130 °C for 15 min to improve crystallinity of P3HT (see the Experimental section). The P3HT–CdSe tetrapod nanocomposites with 80 wt% CdSe tetrapods were used as the photoactive layer after the weight fraction optimization (Fig. S2†). Notably, the 4-azidobenzoic acid-based devices exhibited enhanced power conversion efficiencies (PCEs), approximately three times those of 5-bromovaleric acid-based devices (Fig. 7 and Table 1). The highest performance of the 5-bromovaleric acid-based device was obtained when CdSe tetrapods with a 65 nm stacking height were used. The PCE was 0.471% with a short circuit current, J_{sc}, of 2.78 mJ cm^{-2}, an open circuit voltage, V_{oc}, of 0.659 V, and a fill factor, FF, of 27.9. In sharp contrast, for the same size CdSe tetrapods used, the 4-azidobenzoic acid-based device resulted in a much higher PCE of 1.28% with a J_{sc} of 7.91 mJ cm^{-2}, a V_{oc} of 0.585 V, and a FF of 27.8 under the same fabrication conditions. This clearly demonstrated that aryl molecules possess an efficient charge transfer and transport compared to the alkyl ligands.[31–33] Clearly, the PCE increased from 0.174% to 0.471% and 0.567% to 1.28% for 5-bromovaleric acid-based and 4-azidobenzoic acid-based devices, respectively as the size (*i.e.*, stacking height) of CdSe tetrapods increased from 16 nm to 65 nm (Fig. 7 and Table 1). This can be attributed to the facilitated charge carrier transport due to the extended arm of CdSe tetrapods, considering that the thickness of the photoactive layer was approximately 100 nm. Interestingly, the use of longer (*i.e.*, 94 nm) CdSe tetrapods decreased the performance of the resulting devices regardless of the advantageous size and shape of CdSe tetrapods. This may be ascribed to the local microscopic agglomerations of 94 nm CdSe tetrapods in the P3HT matrix (*i.e.*, the P3HT chains tethered on the surface of tetrapods) (Fig. 8d) due to the decreased solubility of CdSe tetrapods.

In order to investigate the behavior of P3HT–CdSe tetrapod nanocomposites in the P3HT matrix that depends on the weight ratio between P3HT and CdSe tetrapods, P3HT–CdSe tetrapod nanocomposites with different weight fractions of

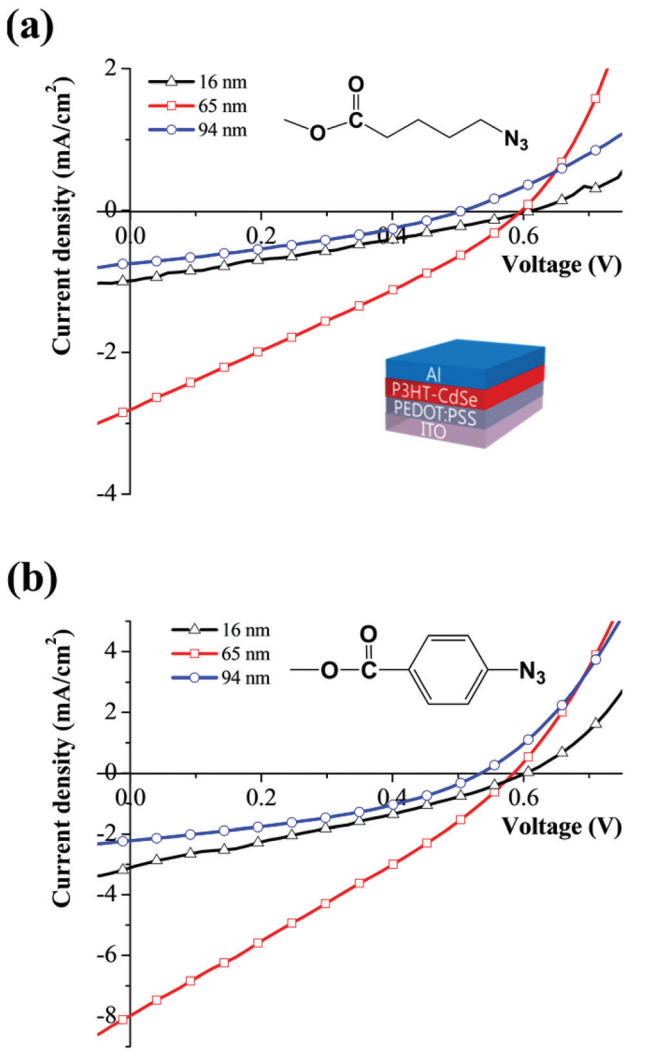

Fig. 7 Current–voltage characteristics of hybrid solar cells composed of P3HT–CdSe tetrapod nanocomposites with the weight fraction of CdSe tetrapods of 80% as photoactive layer. The nanocomposites were synthesized by employing (a) 5-bromovaleric acid and (b) 4-azidobenzoic acid, respectively.

Table 1 Summary of device performances using P3HT–CdSe tetrapod nanocomposites as a photoactive layer synthesized *via* click reaction between P3HT–≡ and 4-azidobenzoic acid (N_3-BA)-capped CdSe tetrapods (left column) and 5-azidovaleric acid (N_3-VA)-capped CdSe tetrapods (right column), respectively. The weight fraction of CdSe tetrapods was 80% for all devices

Ligands	4-Azidobenzoic acid			5-Bromovaleric acid		
Stacking height of tetrapods	16 (nm)	65 (nm)	94 (nm)	16 (nm)	65 (nm)	94 (nm)
V_{oc} (V)	0.604	0.585	0.535	0.624	0.607	0.521
J_{sc} (mA cm^{-2})	3.070	7.910	2.210	0.987	0.278	0.744
FF	30.5	27.8	38.0	28.3	27.9	31.9
PCE (%)	0.567	1.280	0.449	0.174	0.471	0.124

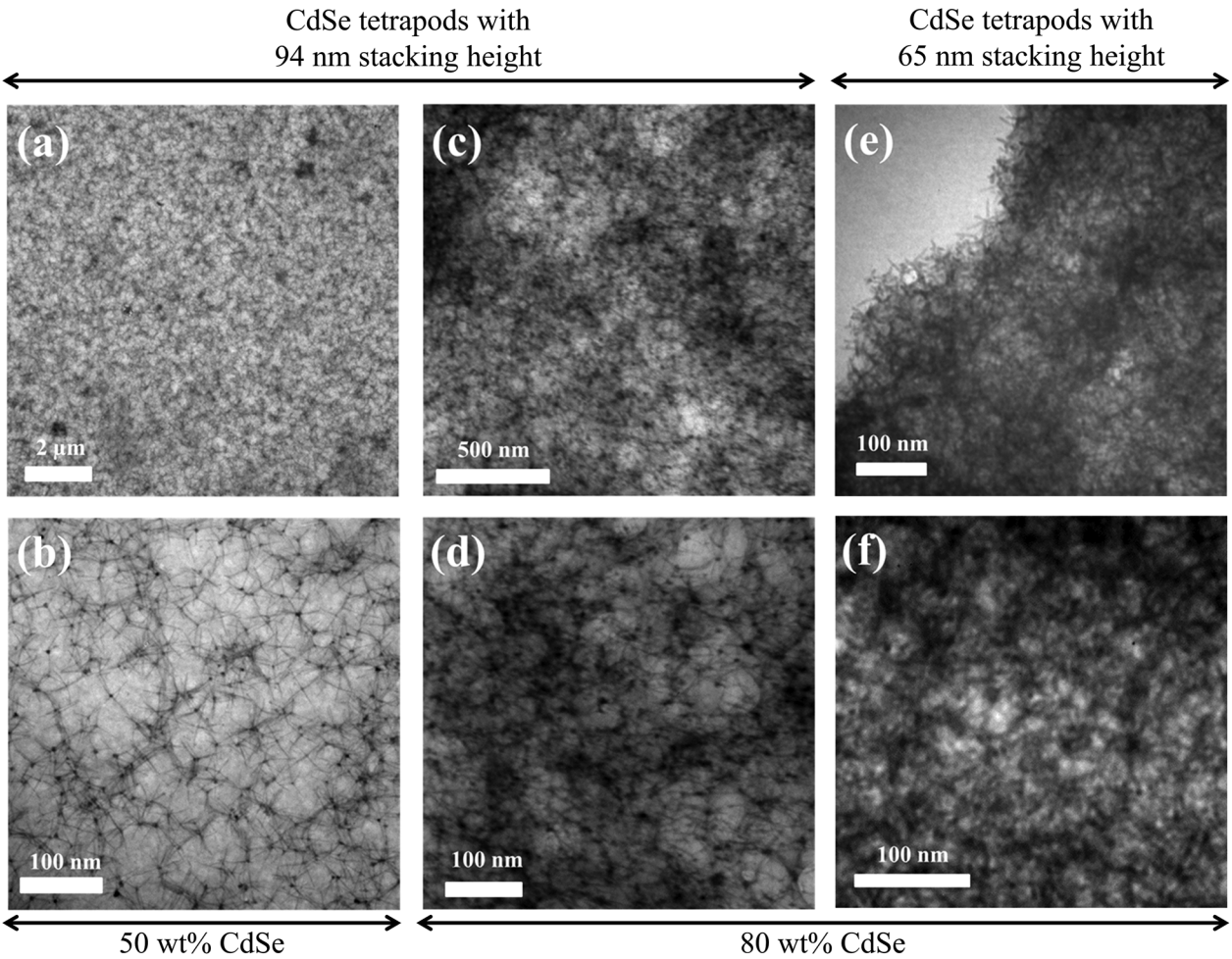

Fig. 8 TEM images of photoactive layer prepared using (a, b) P3HT–CdSe tetrapod nanocomposites with the stacking height of CdSe tetrapods of 94 nm and the weight fraction of 50%, (c, d) P3HT–CdSe tetrapod nanocomposites with the stacking height of CdSe tetrapods of 94 nm and the weight fraction of 80%, and (e, f) P3HT–CdSe tetrapod nanocomposites with the stacking height of CdSe tetrapods of 65 nm and the weight fraction of 80%. In this study, the nanocomposites were synthesized *via* click reaction between P3HT–≡ and 4-azidobenzoic acid (N_3-BA)-capped CdSe tetrapods.

50% and 80% of CdSe tetrapods were synthesized, and the P3HT–CdSe tetrapod nanocomposites films were prepared. TEM studies revealed that P3HT–CdSe tetrapod nanocomposites at 50 wt% of 94 nm CdSe tetrapods were dispersed relatively well in the P3HT matrix (Fig. 8a and b), while increasing the weight fraction of CdSe tetrapod to 80 wt% resulted in the local agglomeration of CdSe tetrapods (Fig. 8c and d). This indicated that the amount of P3HT (20 wt%) was not enough to impart the good dispersion of CdSe tetrapods in the P3HT matrix. Despite the good dispersion of 50 wt% of CdSe tetrapods, the resulting photovoltaic devices did not yield a reasonable performance (*i.e.*, the PCE was 0.077% with a J_{sc} of 1.26 mA cm^{-2}, a V_{oc} of 0.538 V, and a FF of 11.3, Fig. S2†), and even lower than that from P3HT–CdSe tetrapod nanocomposites with 80 wt% of CdSe tetrapods. The morphology of the P3HT–CdSe tetrapod nanocomposite film with 80 wt% of 65 nm CdSe tetrapods was also examined by TEM (Fig. 8e and f). Obviously, the dispersion of relatively small-sized CdSe tetrapods (*i.e.*, 65 nm stacking height) in the P3HT matrix was better than their large counterparts (*i.e.*, 94 nm) at the same weight fraction of CdSe tetrapods. This may lead to an improved PCE for the device fabricated using the 65 nm CdSe tetrapods compared to that from 94 nm CdSe tetrapods.

Conclusion

In summary, semiconducting organic–inorganic nanocomposites comprising conjugated polymers in intimate contact with inorganic tetrapods were crafted *via* a catalyst-free click reaction. CdSe tetrapods were first synthesized from CdSe zincblende seeds by a continuous precursor injection method, followed by a robust inorganic ligand treatment to effectively and completely remove the original insulating fatty ligands on the CdSe tetrapod surface. The subsequent introduction of

short bifunctional ligands formed azide-functionalized CdSe tetrapods. Finally, ethynyl-terminated P3HT was tethered to azide-functionalized CdSe tetrapods *via* a catalyst-free alkyne–azide cycloaddition, yielding intimate semiconducting P3HT–CdSe tetrapod nanocomposites without the presence of any insulating ligands. The success of the click reaction was substantiated by a set of characterization. Compared to the physical mixture of P3HT/CdSe tetrapods, the larger quenching in the emission of P3HT–CdSe tetrapod nanocomposites signified the efficient charge transfer at the P3HT/CdSe tetrapod interface. The scrutiny on the effects of bifunctional ligand types (*i.e.*, aryl *vs.* aliphatic ligands) and the size of tetrapods on the performance of the resulting hybrid solar cells revealed that the aryl bifunctional ligands were more effective in improving device performance than the aliphatic ligands, and CdSe tetrapods with optimal size promoted effective charge transport and good dispersion of CdSe tetrapods, thereby leading to improved device performance. Clearly, the click-reaction strategy enabled by exploiting two consecutive effective ligand exchanges (*i.e.*, inorganic ligand treatment followed by bifunctional ligand exchange) is robust and can be readily extended to produce intimate CP–NC nanocomposites of different compositions and architectures for a wide range of applications in optic, electronic optoelectronic materials and devices.

Experimental section

All chemicals, including cadmium oxide, tri-*n*-octylphosphine (TOP, 90%), selenium powder, sodium azide, 2,5-dibromo-3-hexylthiophene, Ni(dppp)Cl_2, *tert*-butylmagnesium chloride (2 mol L^{-1} in diethyl ether), and ethynylmagnesium bromide (0.5 mol L^{-1} in THF) from Sigma Aldrich; fluoroboric acid (HBF_4), *N*-methylformamide (NMF), and hexane from Alfa Aesar; 4-azidobenzoic acid, 5-bromovaleric acid, 1-octadecene (ODE, 90%), oleic acid (OA, 97%), and cetyltrimethylammonium bromide (CTAB) from TCI were used as received. THF (VWR, 99%) was refluxed over a sodium wire and distilled from sodium naphthalenide solution.

Synthesis of CdSe tetrapods capped with oleic acid

CdSe tetrapods were synthesized *via* a seed-mediated method by modifying the reported synthetic procedure.[14] Zincblende CdSe QDs were prepared as follows. 1 mmol of Se powder and 10 mol of ODE were placed in three neck flask and heated up to 300 °C under Ar. After the solution became clear and transparent, 4 ml of cadmium precursor solution (2 mmol of CdO, 2 ml of OA, and 2 ml of ODE) was injected to initiate nucleation and growth. The resulting CdSe QDs were allowed to grow at 270 °C for 15 min. The heating mantle was then removed to stop the reaction. 6 ml of ODE was added to the solution once the temperature reached 70 °C. The resulting CdSe zincblende solution was used without further purification.

Subsequently, cadmium oleate ($Cd(OA)_2$) precursor solution was prepared by heating 10 mmol of CdO, 7.8 ml of OA, 6.2 ml of ODE, and 1 ml of TOP at 280 °C under Ar for 30 min. Once the solution became colorless and clear, the reaction was cooled down to 50 °C and CTAB (0.14 mmol) and 5 ml of 2 M TOPSe solution was then added and stirred for 10 min.

In order to synthesize CdSe tetrapods, 0.15 μmol of CdSe zincblende seeds were mixed with 1.25 ml of OA, 0.75 ml of TOP, 10.5 ml of ODE, and 0.21 mmol of CTAB. The mixture was then heated to 260 °C, where the precursor solution was injected at the rate of 0.4 ml min^{-1} for 50 min. The heating mantle was removed to stop the reaction, and 5 ml of hexane was then added at 70 °C. An excess amount of acetone was added and centrifuged to purify the resulting solution.

Surface modification of CdSe tetrapods with HBF_4 followed by bifunctional ligands

50 mg ml^{-1} of oleic acid-capped CdSe tetrapods was dissolved in 5 ml of hexane. 0.5 ml of HBF_4 (48 wt% in H_2O) and 5 ml of NMF were added to the CdSe tetrapod solution in hexane. The mixture was then shaken with vortex-mixing for 1 min. The CdSe tetrapods were collected in the polar NMF phase, while oleic acid remained in the nonpolar hexane phase. The hexane phase containing oleic acid was discarded and 5 ml of hexane was added. The oleic acid residue in the NMF phase was washed out *via* vortex mixing. After three repeated washing procedures, the mixture precipitated with an excess amount of acetone. The HBF_4 treatment step was conducted three times in order to completely remove oleate ligands.

To modify bare CdSe tetrapods with bifunctional ligands, HBF_4-treated CdSe tetrapods were precipitated with an excess amount of acetone and redispersed in chloroform containing 5-bromovaleric acid or THF containing 4-azidobenzoic acid to yield 5-bromovaleric acid-capped CdSe tetrapods or 4-azidobenzoic acid-functionalized CdSe tetrapods, respectively. The resulting bifunctional ligand-capped CdSe tetrapod solution was purified with chloroform/acetone or THF/acetone three times to remove the remaining HBF_4. Finally, 5-bromovaleric acid-capped CdSe tetrapods (or 4-azidobenzoic acid-capped CdSe tetrapods) were dispersed in chloroform (or THF).

Synthesis of ethynyl-terminated P3HT

Ethynyl-terminated P3HT (*i.e.*, P3HT–≡) was synthesized by a quasi-living Grignard metathesis (GRIM) method.[34,35] Briefly, 2,5-dibromo-3-hexylthiophene (0.815 g, 2.5 mmol) was dissolved in THF (5 ml) in a three-neck flask and stirred under Ar. *tert*-Butylmagnesium chloride (1.25 ml, 2.5 mmol) was added. The mixture was stirred for 2 h at room temperature. Subsequently, it was diluted to 25 mL with THF, followed by the addition of Ni(dppp)Cl_2 (56 mg, 0.1 mmol). The resulting solution was stirred for 30 min at room temperature, producing intermediate P3HT. It was then reacted with ethynylmagnesium bromide (2 ml, 1 mmol) in THF for 30 min. The product, P3HT–≡, was obtained by precipitating the reaction mixture in methanol, filtering in an extraction thimble, and washing by Soxhlet extraction with methanol, hexane, and chloroform sequentially. It was recovered after the chloroform evaporated.

Synthesis of P3HT–CdSe tetrapod nanocomposites by click reaction

Sodium azide (NaN_3) was added to 5-bromovaleric acid-functionalized CdSe tetrapod THF solution, and then stirred at room temperature for three days, resulting in 5-azidovaleric acid-capped CdSe tetrapods. The excess amount of NaN_3 was removed by centrifugation. The resulting 5-azidovaleric acid-capped CdSe tetrapods were then precipitated with methanol. Subsequently, 50 mg of P3HT–≡ and 50 mg of 5-azidovaleric acid-capped CdSe tetrapod were mixed in 10 ml THF and kept at 65 °C under Ar for two days. For 4-azidobenzoic acid-functionalized CdSe tetrapods, they were directly grafted with ethynyl-terminated P3HT in THF. The final product (*i.e.*, P3HT–CdSe tetrapod nanocomposites) was cooled to room temperature and diluted 10 times with THF. The resulting solution was precipitated with several drops of methanol twice to remove free P3HT which was not coupled with CdSe tetrapods.

Fabrication of P3HT–CdSe tetrapods hybrid solar cells

The solar cells were fabricated as follows. ITO glasses were washed with acetone, methanol, and isopropanol sequentially, followed by oxygen plasma cleaning. Next, a layer of 40 nm thick poly(3,4-ethylenedioxythiophene):poly(styrenesulfonate) (PEDOT:PSS) was spin-cast and annealed at 140 °C for 40 min in air. As-synthesized P3HT–CdSe tetrapod nanocomposites with 50 wt% and 80 wt% of CdSe tetrapods were used without the removal of free P3HT. P3HT–CdSe tetrapod nanocomposites dissolved in chloroform (or chloroform and chlorobenzene mixture) with a concentration of 20 mg ml^{-1} were spin-coated, yielding an approximately 100–200 nm thick photoactive layer, depending on the spin speed. All samples annealed at 130 °C for 15 min and 100 nm of aluminum electrode were deposited with a thermal evaporator at 10^{-6} Torr. All fabrications were done under an inert atmosphere. All devices were characterized at 25 °C under AM1.5 conditions.

Characterization

The morphology of CdSe NCs and P3HT–CdSe tetrapod nanocomposites was studied by using low-resolution and high-resolution transmission electron microscopes (JEOL 100cx and Tecnai F30). The photophysical properties of CdSe tetrapods and P3HT–CdSe tetrapod nanocomposites were explored by using a UV-Vis spectrometer (UV-2600, Shimadzu) and a spectrofluorophotometer (RF-5301PC, Shimadzu). All samples were excited at λ_{ex} = 445 nm and the emissions were collected at λ_{em} > 500 nm. The ^{1}H NMR and Fourier transform infrared (FTIR) spectra were recorded by using a Varian VXR-400 spectrometer.

Acknowledgements

This work is supported by the National Science Foundation (ECCS-1305087) and the Air Force Office of Scientific Research (MURI FA9550-14-1-0037).

References

1 W. U. Huynh, J. J. Dittmer and A. P. Alivisatos, *Science*, 2002, **295**, 2425–2427.
2 Y. Zhou, F. S. Riehle, Y. Yuan, H.-F. Schleiermacher, M. Niggemann, G. A. Urban and M. Kruger, *Appl. Phys. Lett.*, 2010, **96**, 013304.
3 S. Dayal, N. Kopidakis, D. C. Olson, D. S. Ginley and G. Rumbles, *Nano Lett.*, 2009, **10**, 239–242.
4 B. Sun, H. J. Snaith, A. S. Dhoot, S. Westenhoff and N. C. Greenham, *J. Appl. Phys.*, 2005, **97**, 014914.
5 H.-C. Liao, S.-Y. Chen and D.-M. Liu, *Macromolecules*, 2009, **42**, 6558–6563.
6 H. Sirringhaus, N. Tessler and R. H. Friend, *Synth. Met.*, 1999, **102**, 857–860.
7 V. L. Colvin, M. C. Schlamp and A. P. Alivisatos, *Nature*, 1994, **370**, 354–357.
8 W. U. Huynh, J. J. Dittmer and A. P. Alivisatos, *Science*, 2002, **295**, 2425–2427.
9 Q. Sun, Y. A. Wang, L. S. Li, D. Wang, T. Zhu, J. Xu, C. Yang and Y. Li, *Nat. Photonics*, 2007, **1**, 717–722.
10 W. C. W. Chan and S. Nie, *Science*, 1998, **281**, 2016–2018.
11 I. L. Medintz, H. T. Uyeda, E. R. Goldman and H. Mattoussi, *Nat. Mater.*, 2005, **4**, 435–446.
12 V. I. Klimov, A. A. Mikhailovsky, S. Xu, A. Malko, J. A. Hollingsworth, C. A. Leatherdale, H. J. Eisler and M. G. Bawendi, *Science*, 2000, **290**, 314–317.
13 J. Jung, C. H. Lin, Y. Yoon, S. T. Malak, Y. Zhai, E. L. Thomas, V. Vardeny, V. V. Tsukruk and Z. Lin, *Angew. Chem., Int. Ed.*, 2016, DOI: 10.1002/anie.201601198.
14 J. Lim, W. K. Bae, K. U. Park, L. zur Borg, R. Zentel, S. Lee and K. Char, *Chem. Mater.*, 2013, **25**, 1443–1449.
15 Z. Deng, L. Cao, F. Tang and B. Zou, *J. Phys. Chem. B*, 2005, **109**, 16671–16675.
16 S. Asokan, K. M. Krueger, V. L. Colvin and M. S. Wong, *Small*, 2007, **3**, 1164–1169.
17 N. C. Anderson and J. S. Owen, *Chem. Mater.*, 2013, **25**, 69–76.
18 W. Liu, J.-S. Lee and D. V. Talapin, *J. Am. Chem. Soc.*, 2013, **135**, 1349–1357.
19 D. N. Dirin, S. Dreyfuss, M. I. Bodnarchuk, G. Nedelcu, P. Papagiorgis, G. Itskos and M. V. Kovalenko, *J. Am. Chem. Soc.*, 2014, **136**, 6550–6553.
20 H. Zhang, J. Jang, W. Liu and D. V. Talapin, *ACS Nano*, 2014, **8**, 7359–7369.
21 Z. Ning, O. Voznyy, J. Pan, S. Hoogland, V. Adinolfi, J. Xu, M. Li, A. R. Kirmani, J.-P. Sun, J. Minor, K. W. Kemp, H. Dong, L. Rollny, A. Labelle, G. Carey, B. Sutherland, I. Hill, A. Amassian, H. Liu, J. Tang, O. M. Bakr and E. H. Sargent, *Nat. Mater.*, 2014, **13**, 822–828.
22 W. U. Huynh, J. J. Dittmer, W. C. Libby, G. L. Whiting and A. P. Alivisatos, *Adv. Funct. Mater.*, 2003, **13**, 73–79.
23 N. C. Greenham, X. Peng and A. P. Alivisatos, *Phys. Rev. B: Condens. Matter*, 1996, **54**, 17628–17637.
24 J. Lim, D. Lee, M. Park, J. Song, S. Lee, M. S. Kang, C. Lee and K. Char, *J. Phys. Chem. C*, 2014, **118**, 3942–3952.

25 M. T. Khan, A. Kaur, S. K. Dhawan and S. Chand, *J. Appl. Phys.*, 2011, **110**, 044509.
26 J. Jung, X. Pang, C. Feng and Z. Lin, *Langmuir*, 2013, **29**, 8086–8092.
27 M. D. Heinemann, K. von Maydell, F. Zutz, J. Kolny-Olesiak, H. Borchert, I. Riedel and J. Parisi, *Adv. Funct. Mater.*, 2009, **19**, 3788–3795.
28 M. D. Goodman, J. Xu, J. Wang and Z. Q. Lin, *Chem. Mater.*, 2009, **21**, 934–938.
29 L. Zhao, X. Pang, R. Adhikary, J. Petrich, M. Jeffries-EL and Z. Lin, *Adv. Mater.*, 2011, **23**, 2844–2849.
30 L. Zhao, X. Pang, R. Adhikary, J. W. Petrich and Z. Lin, *Angew. Chem., Int. Ed.*, 2011, **123**, 4044–4048.
31 K. E. Knowles, D. B. Tice, E. A. McArthur, G. C. Solomon and E. A. Weiss, *J. Am. Chem. Soc.*, 2010, **132**, 1041–1050.
32 C. Goh, S. R. Scully and M. D. McGehee, *J. Appl. Phys.*, 2007, **101**, 114503.
33 N. Radychev, I. Lokteva, F. Witt, J. Kolny-Olesiak, H. Borchert and J. Parisi, *J. Phys. Chem. C*, 2011, **115**, 14111–14122.
34 R. S. Loewe, P. C. Ewbank, J. Liu, L. Zhai and R. D. McCullough, *Macromolecules*, 2001, **34**, 4324–4333.
35 R. S. Loewe, S. M. Khersonsky and R. D. McCullough, *Adv. Mater.*, 1999, **11**, 250–253.